

AN EXPERIMENTAL INVESTIGATION OF VORTEX

BREAKDOWN ON A DELTA WING*

F. M. Payne and R. C. Nelson
University of Notre Dame
Notre Dame, Indiana

Abstract

An experimental investigation of vortex breakdown on delta wings at high angles is presented. Thin delta wings having sweep angles of 70, 75, 80 and 85 degrees are being studied. Smoke flow visualization and the laser light sheet technique are being used to obtain cross-sectional views of the leading-edge vortices as they break down. At low tunnel speeds (as low as 3 m/s) details of the flow, which are usually imperceptible or blurred at higher speeds, can be clearly seen. A combination of lateral and longitudinal cross-sectional views provides information on the three-dimensional nature of the vortex structure before, during and after breakdown. Whereas details of the flow are identified in still photographs, the dynamic characteristics of the breakdown process have been recorded using high-speed movies. Velocity measurements have been obtained using a laser Doppler anemometer with the 70 degree delta wing at 30 degrees angle of attack. The measurements show that when breakdown occurs the core flow transforms from a jet-like flow to a wake-like flow.

Introduction

The flow structure on the upper side of a delta wing at angle of attack is extremely complex. At moderate angles of attack the leeward flow field is dominated by highly organized vortical flows emanating from the wing leading edge. The vorticity shed from the leading edge rolls up into a pair of primary vortices which can create secondary vortices as illustrated in Figure 1.

One of the most interesting phenomena associated with leading edge vortices is their breakdown. The breakdown or bursting, as it is commonly called, refers to a sudden and rather dramatic structural change which usually results in the turbulent dissipation of the vortex. Vortex bursting is characterized by a sudden deceleration of the axial flow in the vortex core, the formation of a small recirculatory flow region, a decrease in the circumferential velocity and an increase in the size of the vortex.

*This research is being supported by NASA Ames Research Center under NASA Grant NAG-2-258 and the University of Notre Dame. The authors wish to express their appreciation to Dr. Lewis B. Schiff of NASA Ames Research Center for his comments and suggestions during the course of this study. The authors also wish to express their gratitude to Dr. Terry Ng of the Department of Aerospace and Mechanical Engineering of the University of Notre Dame for providing laser Doppler anemometry measurements included in this paper as well as his comments on the interpretation of the flow visualization data.

The breakdown of leading-edge vortices has been under study since the late 1950's when research and design work on delta wing aircraft were initiated. Interest in the phenomenon has intensified in recent years as concepts for highly maneuverable aircraft have been developed. These high-performance aircraft are expected to operate routinely at angles of attack at which vortex breakdown is known to occur.

Several distinct types of vortex breakdowns have been identified in vortex tube experiments (Ref. 1); however, the two most common forms of breakdown on wings are the bubble and spiral types. The bubble or "axisymmetric" mode of vortex breakdown is characterized by a stagnation point on the swirl axis, followed by an oval-shaped recirculation bubble. The bubble is nearly symmetric over most of its length, but the rear is open and asymmetric (Figure 2).

The spiral mode of breakdown is characterized by a rapid deceleration of the core flow followed by an abrupt kink at which point the core flow takes the form of a spiral which persists for one or two turns before breaking up into large scale turbulence (Figure 3a). For leading-edge vortices the sense of the spiral winding has been observed to be opposite to the direction of rotation of the upstream vortex; however, the sense of rotation of the winding is in the same direction as the rotation of the upstream vortex (Figure 3b).

In vortex tube experiments in which the vortex swirl speed can be controlled and varied independently of Reynolds number (Ref. 1), the spiral type has been found to occur at low values of swirl for a given Reynolds number. As the swirl speed is increased the spiral form can be seen to transform into the bubble form at a certain critical value of swirl.

While the bubble type breakdown has been observed on delta wings in low Reynolds number water tunnel studies (Ref. 2), it is the spiral type which is more commonly observed in wind tunnel studies.

A wind tunnel smoke flow visualization study is described herein. Four delta wings with sweep angles of 70, 75, 80 and 85 degrees were tested at angles of attack from 10 to 40 degrees. The freestream velocity was 3 m/s. A low freestream velocity was chosen because details of the flow can be seen which are imperceptible at higher speeds.

Velocity profiles are presented for the leading-edge vortex on a 70 degree delta wing at 30 degrees angle of attack and a freestream velocity of 9.1 m/s. The axial and swirl velocity components were obtained in separate test runs using a single component laser. Since a frequency shifting unit was not available at the time of the test only the absolute value of the velocity was measured.

Experimental Equipment

All experiments reported on in this paper were conducted in the University of Notre Dame's low turbulence, subsonic smoke wind tunnel. The tunnel is of the indraft variety and is shown in Figure 4. Twelve anti-turbulence screens are located in front of a 24:1 area contraction cone. The combination of anti-turbulence screens and the large inlet contraction provides a uniform velocity profile with a turbulence intensity of less than 0.1% in the tunnel test section.

The test section is 1820mm long with a 610 x 610mm square cross section. The test section was designed with large plate glass windows in the top and both sides of the section to provide adequate viewing area for the visualization studies. Following the test section, the flow is expanded in a diffuser. The tunnel is powered by an eight-bladed fan and an 11kw AC induction motor located at the end of the diffuser section.

For visualization, smoke was generated by the flash vaporization of deodorized kerosene which was allowed to drip onto electrically heated plates. The smoke was pushed through the generator and into the smoke rake by a small squirrel cage blower. Figure 5 is a sketch of the smoke generator. The smoke rake consists of a heat exchanger, filter bag and smoke tubes. For this study, the smoke was introduced via a single tube as illustrated in Figure 6.

Four thin plexiglass delta wing models were used in this study. The models each had a root chord of 406mm and were 6.4mm thick with sweep angles of 70, 75, 80, and 85 degrees. The leading edge was beveled with a 25 degree angle. The models were sting mounted to a support system that provided very little interference to the flow.

To illuminate the smoke entrained into the leading-edge vortex system a laser light source was used. During the course of this study two different lasers were used. A Lexel Model 95, 8 watt argon ion laser and a Spectra Physics model 164, 4 watt argon ion laser were used in conjunction with a splitter lens having either a 20 degree or 60 degree spreading angle. The lens created a thin light sheet which passed through the test section. The laser light sheet was aligned either normal to the model surface or parallel to the vortices.

Both still and high-speed motion picture photography were used to record the visual data. A Nikon FM2, 35mm SLR camera and Kodak Tri-X 400 ASA black and white print film were used for the still photographs. For the high-speed movies a Milliken DBM-5, 16mm motion picture camera was used. Film frame rates of 500 frames per second (shutter speed 1/1300 sec) were used with Eastman 4-X Negative film.

Several preliminary experiments using a single component laser anemometer have been conducted using the 70 degree swept delta wing. The laser anemometer system consisted of a 4 watt argon ion laser (an output level of about 1 watt was obtained when operated with the 514.5mm line), a 50mm beam splitter and a 500mm focal length lens as the transmitting optics, and a receiving optics in an off-axis, forward scattering configuration. Kerosene smoke was used as the scattering particles. The signal was processed by a counter and the data were recorded by a data acquisition system based on a PDP 11/23 minicomputer.

Experimental Results

Flow Visualization Results

Smoke flow visualization and the laser sheet technique were used to study the structure of leading-edge vortices as they break down. Figure 7 is a sketch of the experimental setup. At low freestream velocities (as low as 3 m/s), details of the flow can be clearly seen which are usually imperceptible at higher speeds. A combination of lateral and longitudinal laser cross-sectional views provides

information on the three-dimensional nature of the vortex structure before, during and after breakdown. Close-up high-speed motion picture photography provides details of the dynamic characteristics of the breakdown process. An attempt is made to classify the observed breakdown modes using these methods.

Four thin sharp-edged delta wings with sweep angles of 70, 75, 80 and 85 degrees were photographed at angles of attack of 10, 20, 30 and 40 degrees. Vortex breakdown was observed to occur above all four wings at 40 degrees angle of attack. Since vortex breakdown is the phenomenon of primary interest here, only the results at 40 degrees angle of attack for each wing will be presented.

Early in the investigation it was discovered that operating at relatively low speeds resulted in better resolution of flow features due to a reduced level of turbulence in the test section and a higher density of smoke. For this reason a freestream velocity of 3 m/s was chosen for all flow visualization tests. This resulted in a Reynolds number based on root chord of approximately 85,000.

One notable consequence of operating at very low speeds was the tendency of the position of the breakdown to wander on the more highly swept wings. For the lowest sweep wing (70 deg), the breakdown locations of the vortices were approximately symmetric and steady except for a high-frequency longitudinal oscillation about some mean position. The magnitude of this oscillation was relatively small (about 1 cm). On the more highly swept wings the locations of the breakdowns became increasingly asymmetric and unsteady in their mean location. On the 85 degree sweep wing the breakdown location of both vortices was observed to wander forward and aft on the model apparently at random. However, if the tunnel speed was increased (to say 15 m/s) the unsteadiness in mean position disappeared although the breakdown positions still tended to be asymmetric. No measurable asymmetry could be identified in the model geometry; however, the accuracy in measurement of yaw angle was approximately 1/2 degree which could account for the asymmetric breakdown if the model was misaligned by that amount. In wind tunnel tests of highly swept delta wings (75-85 deg) at a Reynolds number of 1×10^6 , Wentz (Ref. 3) observed that the breakdown location was quite sensitive to yaw. A misalignment of as little as 0.1 degrees was sufficient to cause asymmetric breakdown. The location of breakdown at 15 m/s for the four wings tested is presented in Figure 8.

In summary, the wandering of the mean location of breakdown on the 80 and 85 degree wings occurred only at low speeds but the asymmetry in mean breakdown location for those wings occurred at both low (3 m/s) and relatively high (15 m/s) speeds. The low-magnitude, high-frequency oscillation of the breakdown location occurred for all wings at all speeds tested.

Figure 9a depicts the geometry of the 70 degree wing. Figure 9b is a photograph of this model at 40 degrees angle of attack. A tube of smoke introduced upstream of the contraction cone impinges on the apex of the delta wing and is entrained into the vortices. A 1000 watt flood lamp placed outside the test section is illuminating the vortices through the glass side wall of the test section. Both vortices are breaking down about 1/3 of the way down the model from the apex.

Figure 9c is a multiple exposure photograph of the 70 degree delta wing using the laser sheet technique. Vortex cross sections are illuminated by passing the

laser beam through a cylindrical lens which splits it into a thin sheet or plane of light. The light sheet then cuts across the test section. In this case the sheet is perpendicular to the model. The light sheet is expanding at a half angle of approximately 10 degrees.

Note the absence of smoke in the core region of the vortices in the two most forward cross sections of Figure 9c. This lack of smoke can probably be attributed to one or more of the following factors. (1) The smoke is introduced only at the apex of the model, therefore, much of the fluid in the core region is entrained from areas which contain no smoke to begin with. (2) Velocities in the core can reach three to five times the freestream value which reduces the density of smoke entrained into the core. (3) High rotational velocities in the core tend to "spin" smoke particles out.

The first reason may be the most significant because the diameter of the region which is void of smoke was observed to vary depending on where the smoke filament impinged on the model. If the filament impinged on the lower surface below the apex, the void region was seen to increase in diameter. Despite the fact that the void may not correspond to the true diameter of the core, for the sake of simplicity, it will be referred to as the core in the remainder of this paper.

In the forward cross sections of Figure 9c, the presence of a core indicates that the vortex has not yet broken down. In the third and following cross sections, which are downstream of the breakdown points, no core regions are evident and the vortices appear turbulent and diffuse.

Figure 9d is a photograph of the 70 degree wing at the same conditions as previously stated except that the laser sheet has been rotated 90 degrees to illuminate a longitudinal cross section of the vortices. The dark core region maintains an approximately constant diameter until suddenly expanding just before breaking down. Downstream of the breakdown the vortices are rather featureless.

Figures 10, 11 and 12 present similar views of the 75, 80 and 85 degree wings respectively. Note that the breakdown occurs farther aft as the sweep angle is increased. Also note the fine details visible in the photographs of the 85 degree delta wing. The high sweep angle results in lower swirl velocities and therefore less diffusion of the smoke.

In Figure 12b the spiral nature of the vortices is visually emphasized by the appearance of striations in the smoke. The striations become visible when the flow is accelerated around the leading edge and the smoke mixes with entrained flow in the vortex. In this photograph the vortex on the right is breaking down at approximately the mid-chord position while the left vortex does not break down until somewhere in the wake. The combination of high sweep and low freestream velocity usually resulted in asymmetric vortex breakdown as previously discussed. Which vortex would breakdown first could not be predicted and was observed to change back and forth at irregular intervals. This was probably the result of small changes in the freestream conditions due to gusts or changes in the direction of the wind at the tunnel exit.

In Figure 12c it is possible to actually see the roll-up of the shear layer which forms the primary vortices and the development of secondary vortical-like

structures in the shear layer. The growth of these secondary structures is similar to the evolution of the classic Kelvin-Helmholtz instability. Gad-el-Hak and Blackwelder (Ref. 4) similarly observed the development of secondary vortical-like structures in a towing tank experiment with a 60 degree delta wing. In their experiments, which were conducted at a Reynolds number of 13,000 and also employed the laser sheet technique, dye injected near the leading edge was observed to roll-up into regions of strong concentration separated by a very thin braid of dye. These concentrated regions in the shear layer were assumed to be discrete vortices. The fact that these structures have been identified in both tow tank experiments using dye injection and wind tunnel experiments using smoke suggests that the observed structures are indeed associated with the flow and are not merely a consequence of the visualization method.

In Figure 12d it is the right vortex which is breaking down. Details in the recirculation zone or "bubble" region are clearly visible. Note that the vortices curve slightly away from the wing ("out" of the photograph) and since the laser sheet is planer, the laser cross section cuts at an angle through the vortices. This is why the core region is only visible for a portion of the entire cross section. The direction of the spiral on the right side of the lower vortex indicates the laser sheet is cutting across the underside of the vortex at that point.

An extremely useful tool in the analysis of complicated flows is the motion picture camera. In order to obtain a better understanding of the breakdown structure, a Milliken high-speed movie camera was used to photograph the phenomenon at 500 frames per second. The effective shutter speed for a single frame was 1/1300 of a second. In Figures 13-16, single frames from the 16mm movies have been isolated and enlarged. The photographs are longitudinal and lateral laser sheet cross sections of vortex breakdown on the 85 degree delta wing. Accompanying the photographs are sketches depicting the salient features observed in the movie frames.

One of the goals of this study is to identify the type or types of breakdowns which occur on sharp-edged delta wings at these Reynolds numbers; however, a certain amount of caution must be exercised when interpreting flow visualization results. What is not seen may be just as important as what is seen. The still photographs described above, together with the high-speed motion pictures, can be interpreted in various ways. The particular ambiguity which makes a definite identification of the breakdown process difficult in this case is that the smoke in these photographs is entrained into the outer region of the vortex and not into the core and it is the behavior of the core which is of primary interest. The core behavior must be inferred by observing a region void of smoke. With this difficulty in mind two possible breakdown forms will be described.

The first type of breakdown process resembles the bubble form described in vortex tube experiments found in the literature. In Figure 13 the core flow seems to expand around an oval shaped recirculation zone. At the exit of this recirculation zone the core flow appears to shed in the form of vortex rings which are then convected downstream. The cross section of these doughnut shaped vortex rings appears as a pair of holes in the smoke. Figure 14 shows a lateral cross section of the recirculation zone which is surrounded by a ring of core flow.

The breakdown process described was occasionally observed to change into what might be interpreted as a spiral mode. When this occurred the mean location of the breakdown moved downstream and took the form depicted in Figure 15. The large recirculation zone has disappeared and the core flow now appears to corkscrew downstream. In this case the holes in the flow are assumed to be cross sections of the spiraling core flow. This type of result was also obtained in wind tunnel tests at ONERA using the laser sheet technique (Ref. 5). In that study "holes" appearing in the wake of a breakdown were also observed and interpreted to be cross sections of the spiraling vortex core. Figure 16 shows a lateral cross section which appears to show a rotating core. After a short time this spiral mode would transform back into the "bubble" form and move upstream.

Further experiments are planned to verify one or both of the above descriptions of breakdown modes. In particular an attempt will be made to introduce smoke into the vortex core from a port in the surface of the model.

LDA Measurements

A laser anemometer was used to measure the axial and normal components of velocity through the vortex core of the 70 degree delta wing at 30 degrees angle of attack.

An example of these preliminary measurements is shown in Figure 17. This figure shows the change in axial velocity distribution before and after vortex breakdown. Breakdown of the vortex occurred between stations $x/c = 0.47$ and $x/c = 0.54$. The axial velocity upstream of the vortex breakdown point is over three times the freestream velocity in the vortex core. However, the wake survey made just downstream of the breakdown shows a region of velocity deficit with respect to the surrounding flow.

The time required for a traverse of the vortex depended on the number of samples acquired at each point, the number of scattering particles in the flow, movement of the instrument to the next point, and the total number of points in the traverse. Thus, the LDA results represent a time average of the flow characteristics and do not entirely reflect the complicated nature of the breakdown region. Nevertheless, valuable insight is gained from the average velocity profiles.

Figure 18 shows the change in swirl velocity at various positions along the wing. Again we see a dramatic change in swirl velocity after breakdown has occurred.

Conclusions

Smoke flow visualization and the laser sheet technique have been shown to be effective tools in the study of vortical flow fields. The position of leading-edge vortices and the location of their breakdown at high angles of attack can be determined. Details of the breakdown process have been studied using still and high-speed motion picture photography.

The following observations were made concerning vortex breakdown on delta wings at low Reynolds number:

(1) At a given angle of attack, as the sweep angle is increased, the location of breakdown moves aft.

(2) For a given set of conditions the breakdown location oscillated at high frequency about a mean position and for highly swept wings (sweep = 80, 85 deg) at low speeds the mean position would migrate considerably forward and aft on the models.

(3) High-speed motion pictures revealed what appears to be two types of breakdown on the 85 degree wing, a bubble mode and a spiral mode. The two modes were seen to transform from one to the other apparently at random with the bubble form seeming to prefer a more upstream location relative to the spiral mode. The existence of more than one mode of breakdown as well as their behavior with respect to preferred location is consistent with observations of vortex breakdown in tubes reported in the literature.

(4) Velocity profiles obtained with a laser anemometer showed the development of a jet-like core flow which reached three times the freestream velocity before breaking down. After the breakdown the velocity profiles became wake-like in nature.

References

1. Faler, J. H. and Liebovich, S., "Disrupted States of Vortex Flow and Vortex Breakdown," Phys. Fluids 20, 1977, 1385-1400.
2. Lambourne, N. C. and Bryer, D. W., Aeronaut. Res. Council., "The Bursting of Leading Edge Vortices; Some Observations and Discussion of the Phenomenon," R & M No. 3282, 1961, 32 pp.
3. Wentz, W. H. and Kohlman, D. L., "Vortex Breakdown on Slender Sharp-Edged Wings," Journal of Aircraft, Vol. 8, No. 3, March 1971.
4. Gad-el-Hak, M. and Blackwelder, R. F., "The Discrete Vortices from a Delta Wing," AIAA Journal, Volume 23, No. 6, June 1985.
5. Werle, H., "Flow Visualization Techniques For the Study of High Incidence Aerodynamics," AGARD LSP-121, March 1982, Paper 3-1 to 3-24.

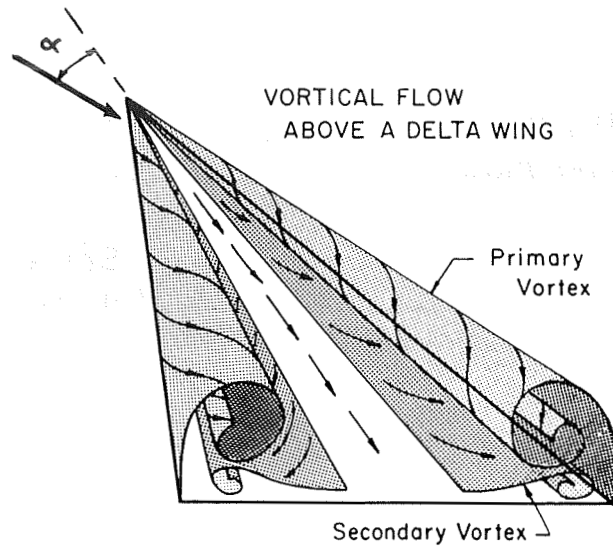


Figure 1. Flow over a delta wing.

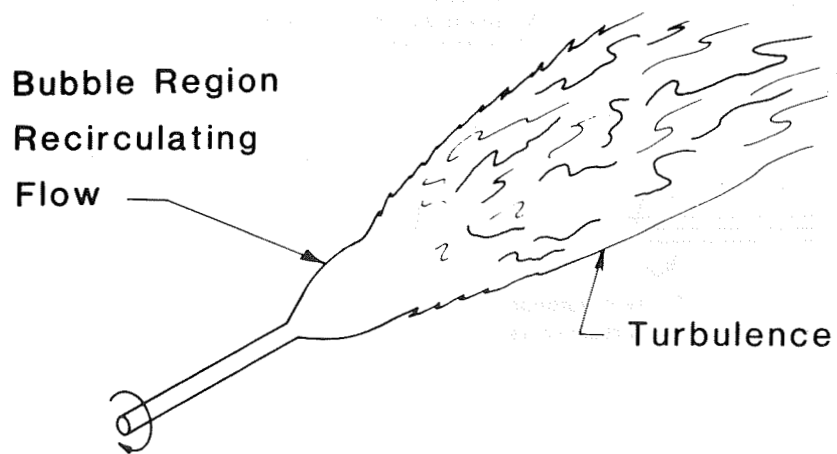
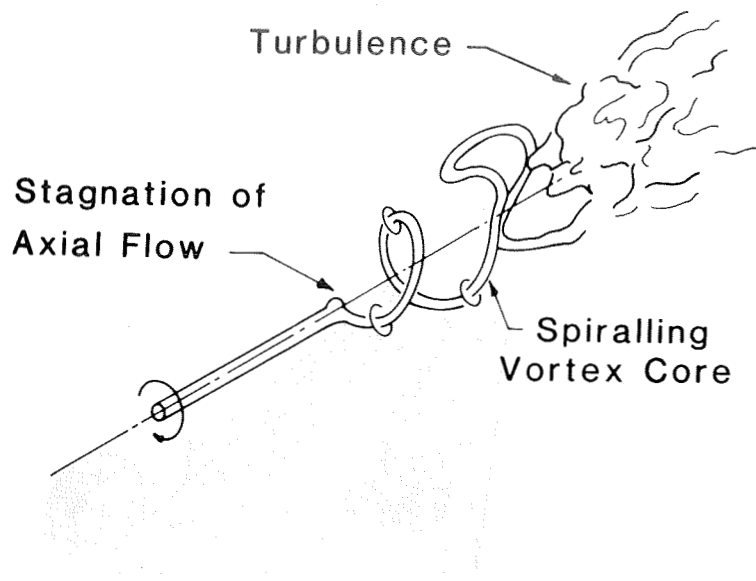
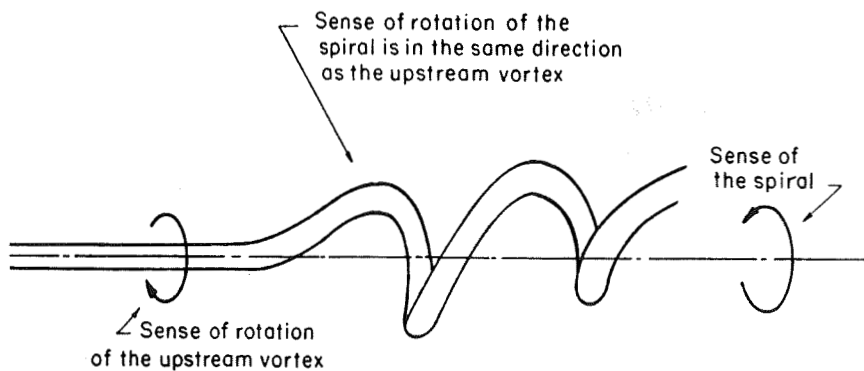


Figure 2. Bubble-type breakdown.



a. Spiral-type breakdown.



b. Sense of rotation of the spiral.

Figure 3. Spiral-type breakdown and sense of rotation of spiral.

ORIGINAL PAGE IS
OF POOR QUALITY

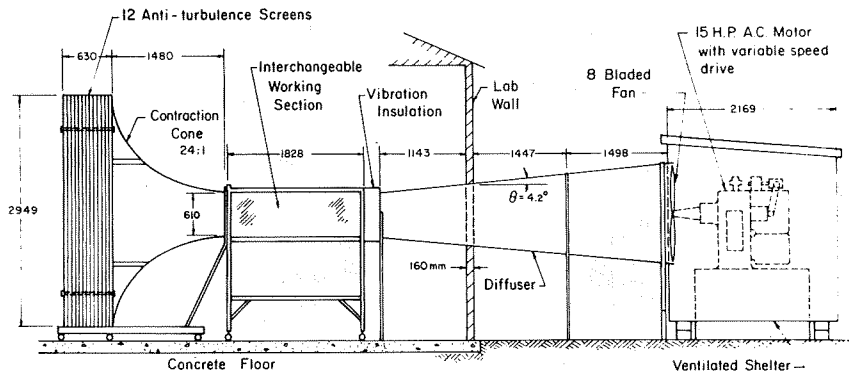


Figure 4. Schematic of wind tunnel.

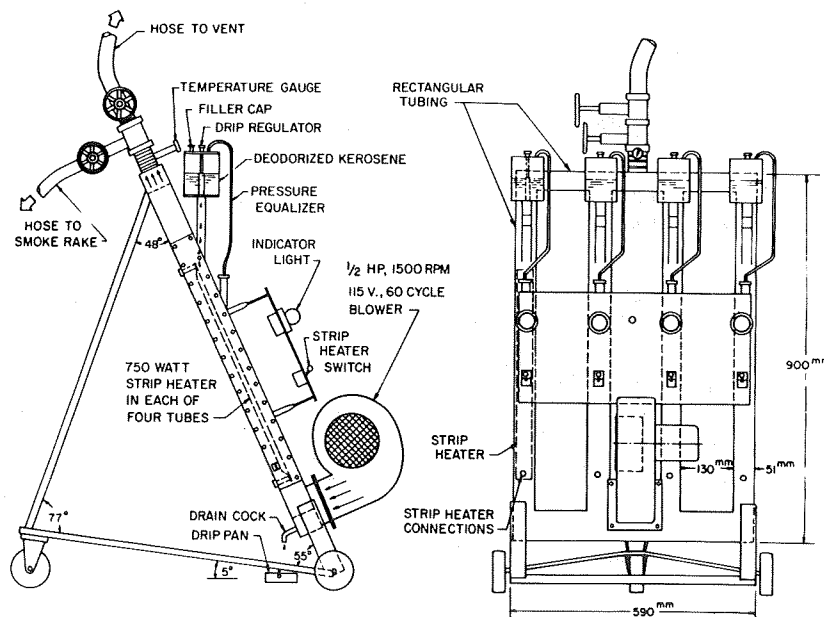


Figure 5. Schematic of smoke generator.

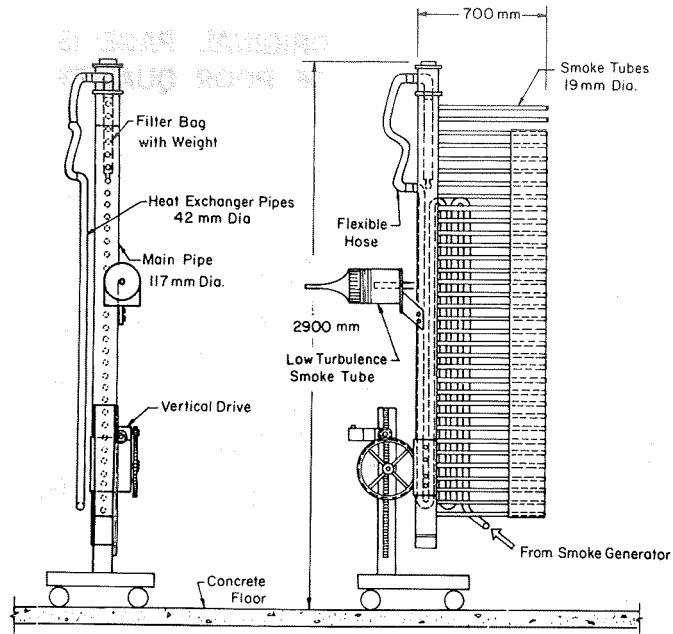


Figure 6. Schematic of smoke rake.

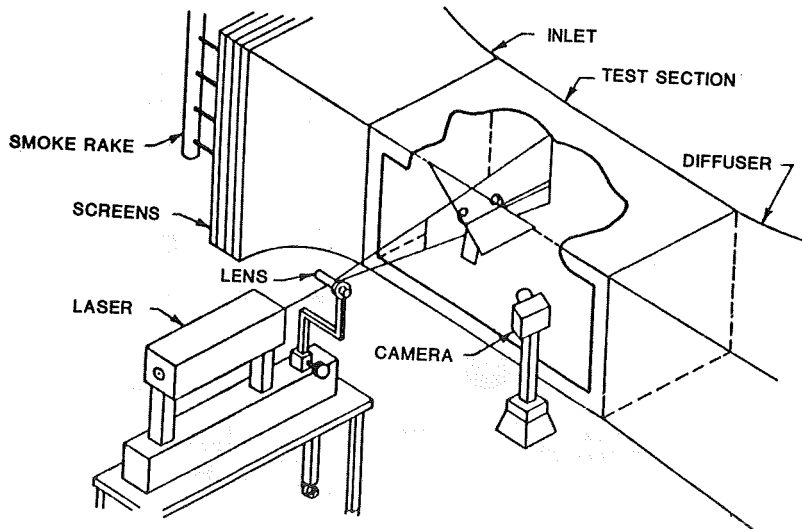


Figure 7. Schematic of experimental setup.

LOCATION OF VORTEX BREAKDOWN

Re = 425,000

- $-\Lambda = 70^\circ$
 - $-\Lambda = 75^\circ$
 - △ $-\Lambda = 80^\circ$
 - ◇ $-\Lambda = 85^\circ$
- Left Vortex
 - - - Right Vortex

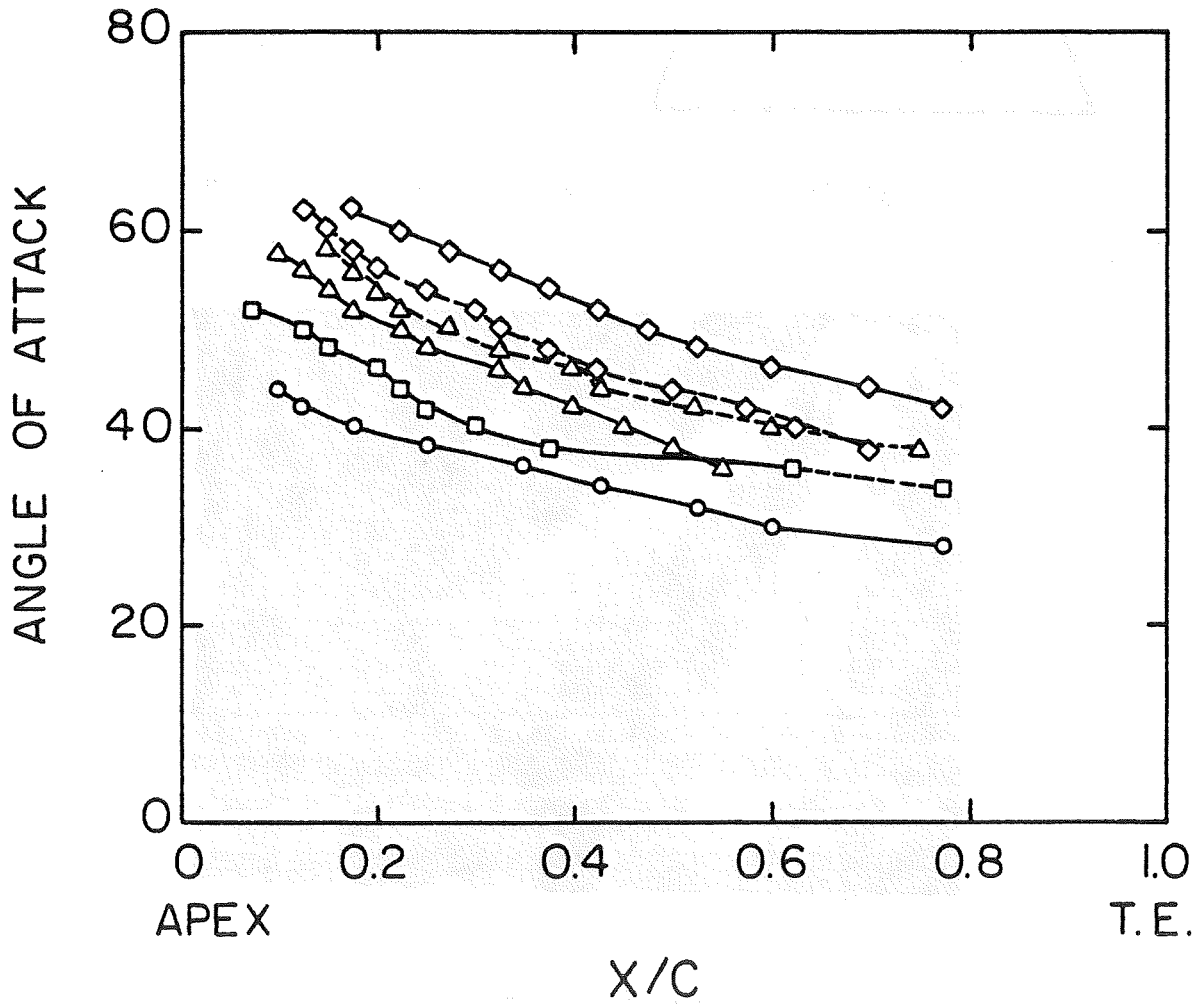
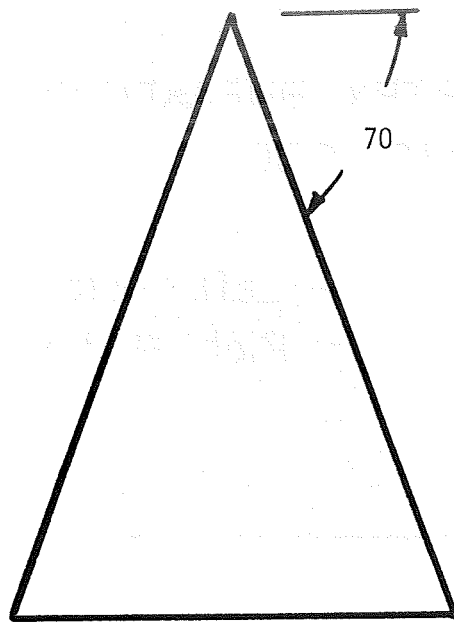



Figure 8. Location of vortex breakdown.



Planview of Model

 LE = 70 degrees

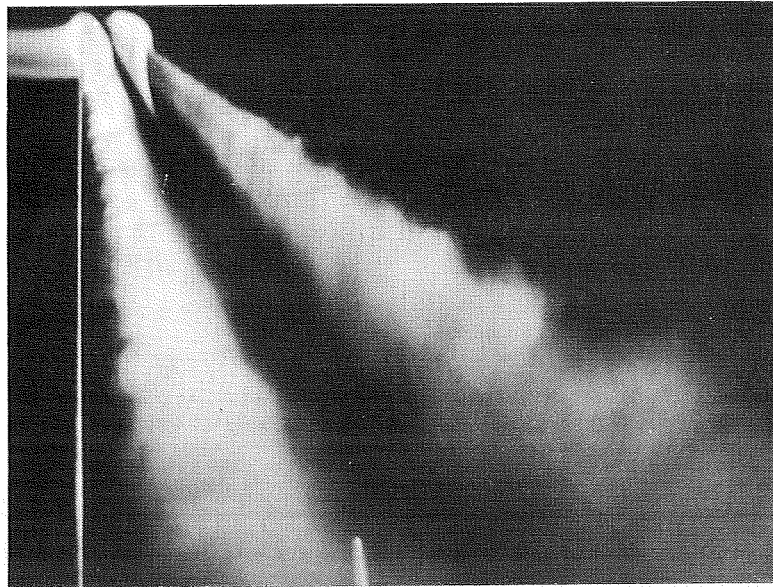
$c = 406\text{mm}$

AR = 1.46

$t/c = 0.016$

Beveled leading edge -25 degrees

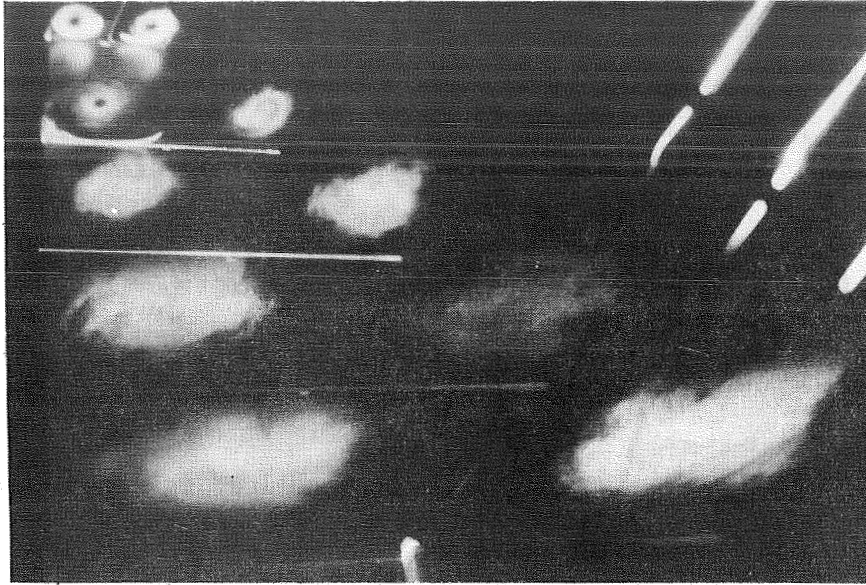
a. Geometry of 70-degree swept delta wing.



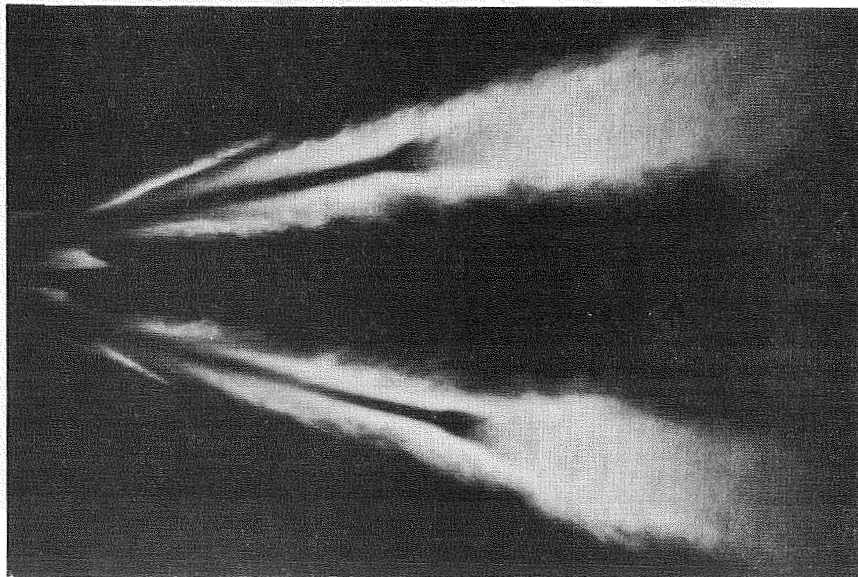
b. Smoke flow visualization with flood lamp illumination. Sweep = 70 deg, Alpha = 40 deg, $V_{\infty} = 3\text{ m/s}$.

Figure 9. 70-degree swept delta wing.

ORIGINAL PAGE IS
OF POOR QUALITY

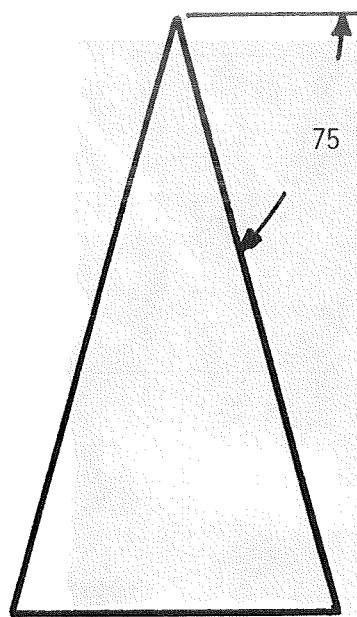


- c. Lateral laser sheet cross sections.
Sweep = 70 deg, Alpha = 40 deg, $V_{\infty} = 3$ m/s.



- d. Longitudinal laser sheet cross section.
Sweep = 70 deg, Alpha = 40 deg, $V_{\infty} = 3$ m/s.

Figure 9. Concluded.



Planview of Model

\angle LE = 75 degrees

$c = 406\text{mm}$

$AR = 1.07$

$t/c = 0.016$

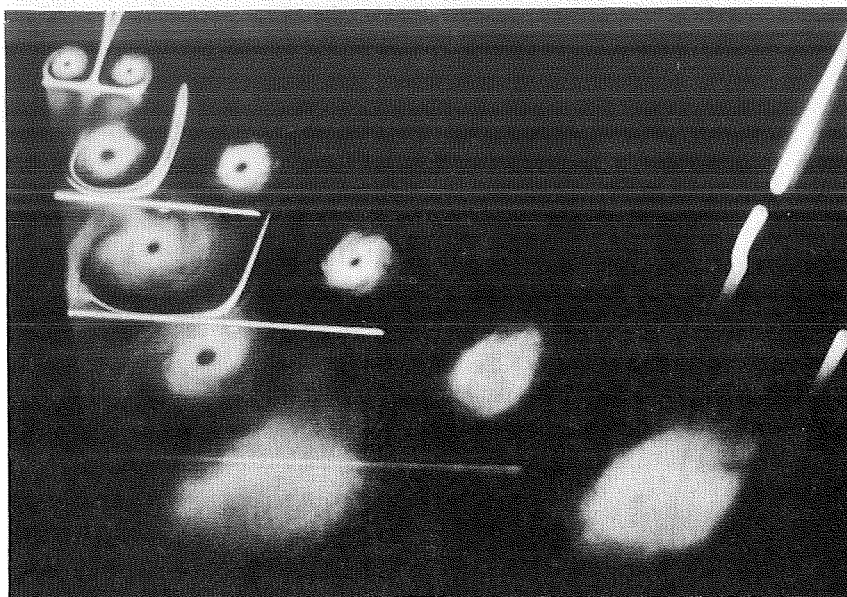
Beveled leading edge -25 degrees

a. Geometry of 75-degree swept delta wing.

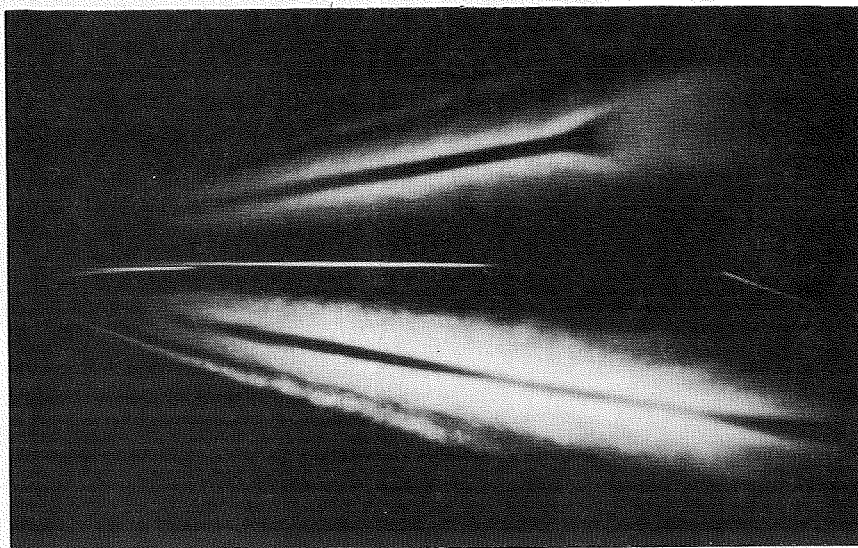


b. Smoke flow visualization with flood lamp illumination. Sweep = 75 deg, $\alpha = 40$ deg, $V_\infty = 3$ m/s.

Figure 10. 75-degree swept delta wing.

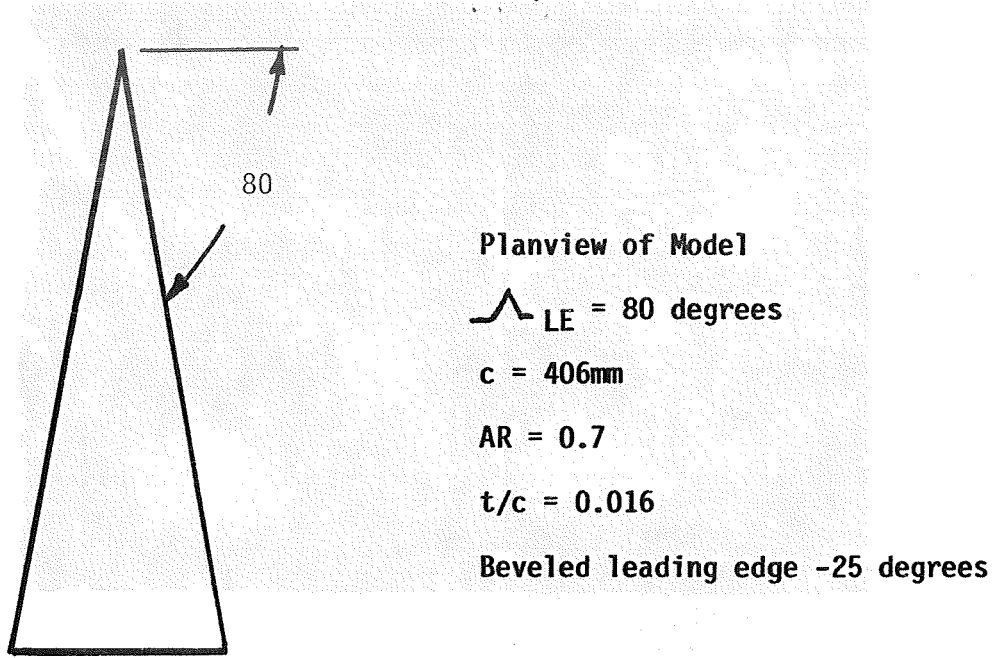


c. Lateral laser sheet cross sections.
Sweep = 75 deg, Alpha = 40 deg, $V_{\infty} = 3$ m/s.

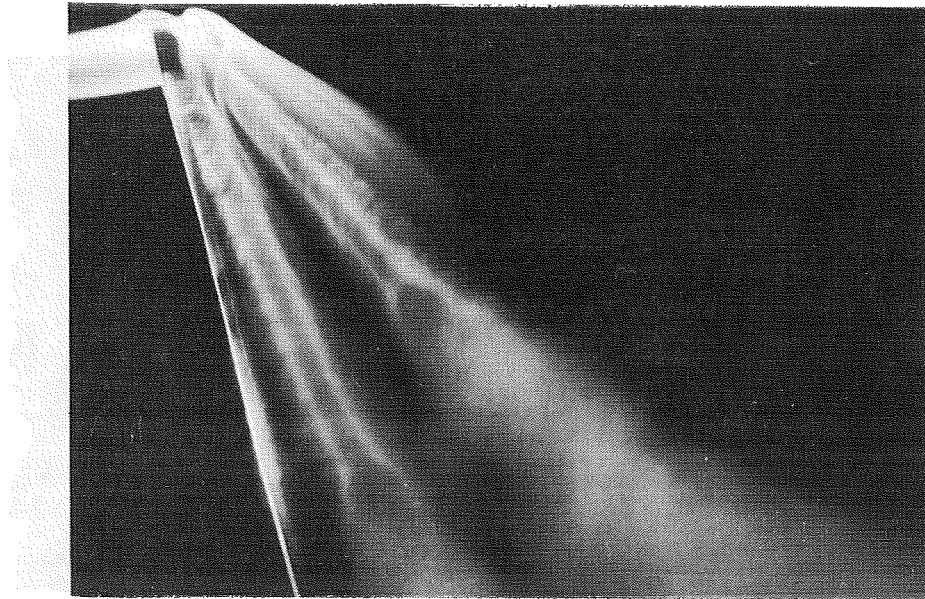


d. Longitudinal laser sheet cross section.
Sweep = 75 deg, Alpha = 40 deg, $V_{\infty} = 3$ m/s.

Figure 10. Concluded.



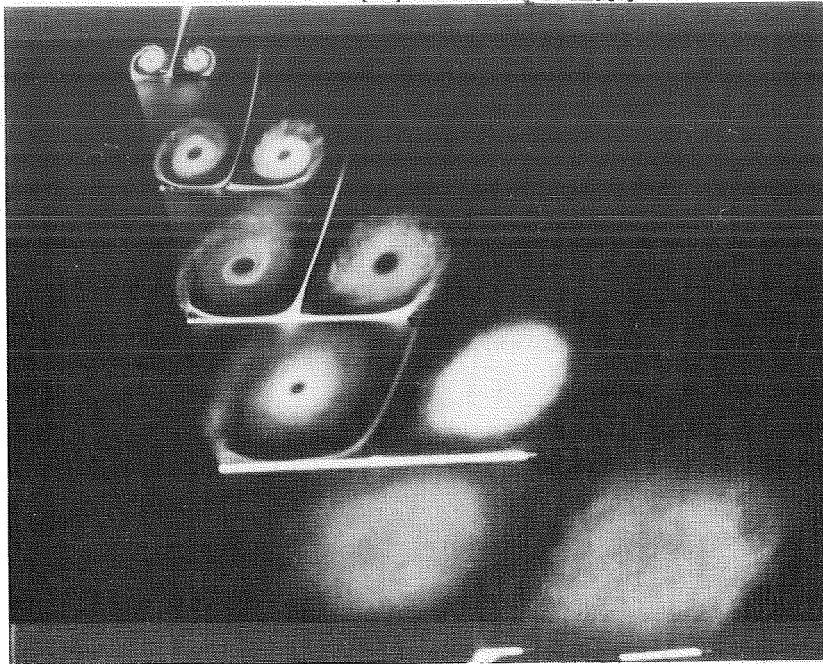
a. Geometry of 80-degree swept delta wing.



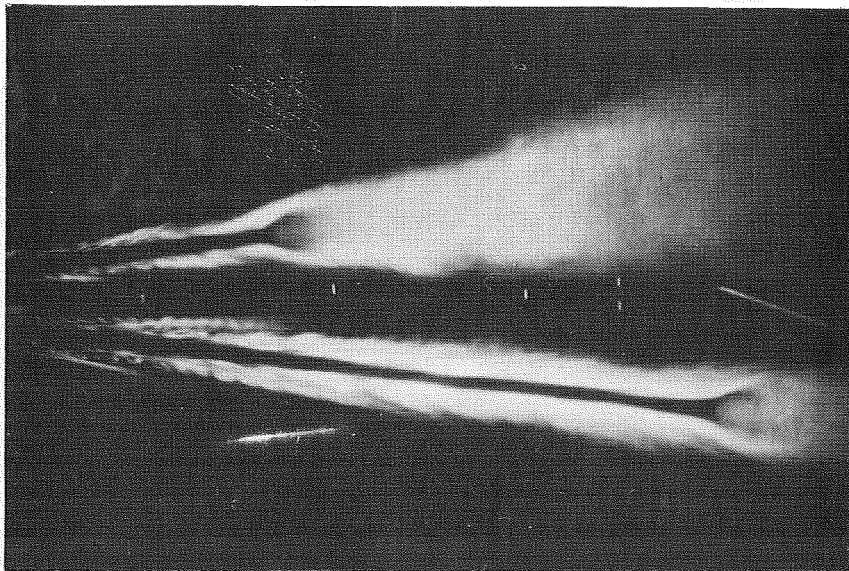
b. Smoke flow visualization with flood lamp illumination. Sweep = 80 deg, $\alpha = 40$ deg, $V_\infty = 3$ m/s.

Figure 11. 80-degree swept delta wing.

ORIGINAL PAGE IS
OF POOR QUALITY

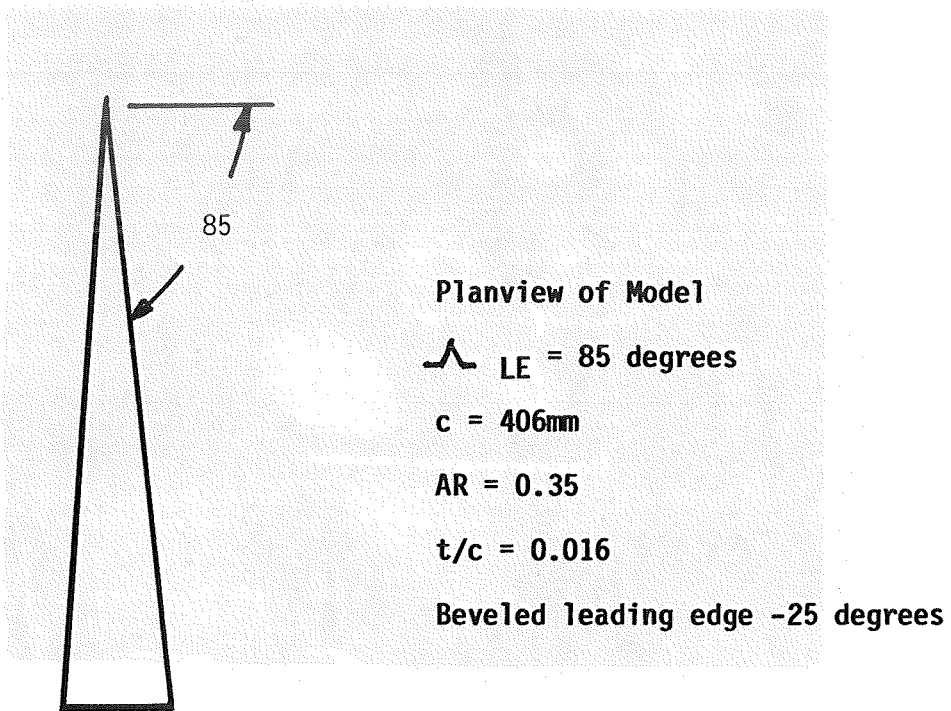


c. Lateral laser sheet cross sections.
Sweep = 80 deg, Alpha = 40 deg, $V_{\infty} = 3$ m/s.

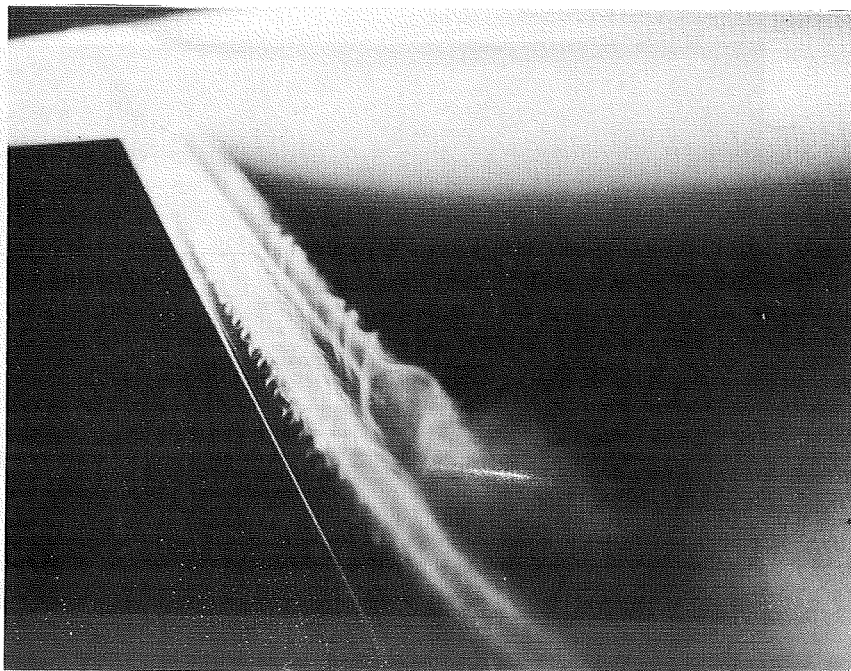


d. Longitudinal laser sheet cross section.
Sweep = 80 deg, Alpha = 40 deg, $V_{\infty} = 3$ m/s.

Figure 11. Concluded.



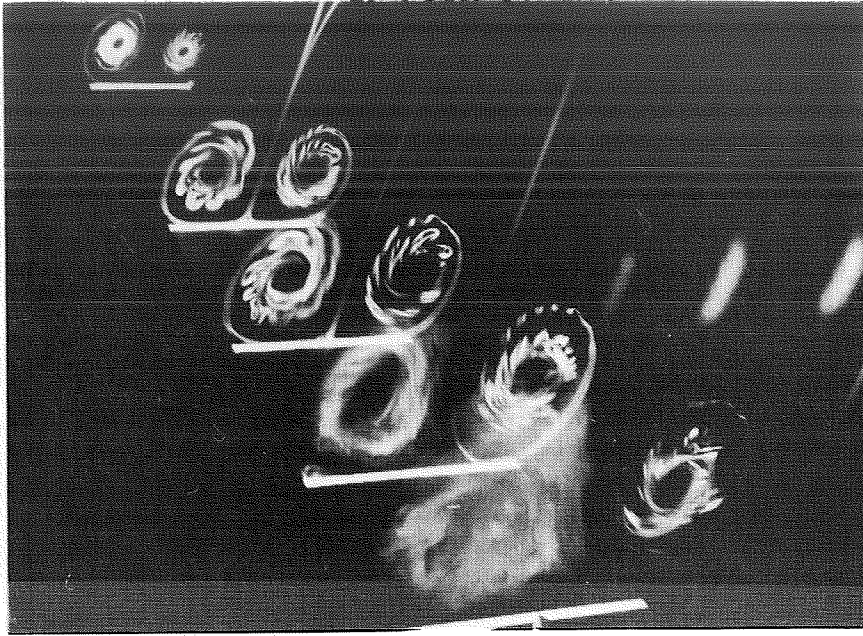
a. Geometry of 85-degree swept delta wing.



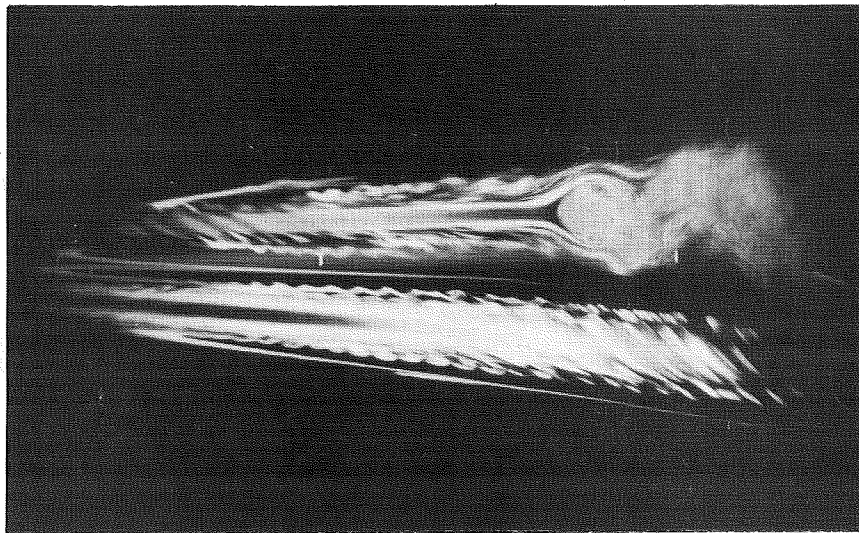
b. Smoke flow visualization with flood lamp illumination. Sweep = 80 deg, $\alpha = 40$ deg, $V_\infty = 3$ m/s.

Figure 12. 85-degree swept delta wing.

ORIGINAL PAGE IS
OF POOR QUALITY

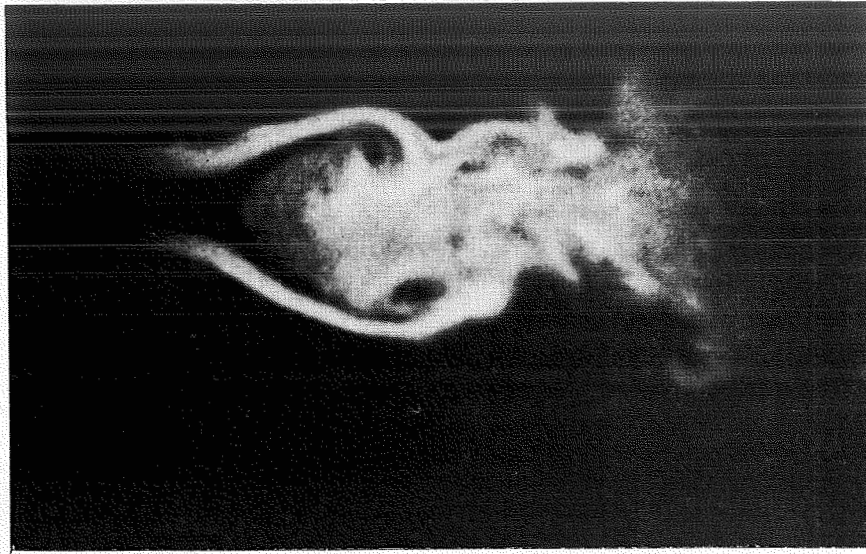


c. Lateral laser sheet cross sections.
Sweep = 85 deg, Alpha = 40 deg, $V_{\infty} = 3$ m/s.

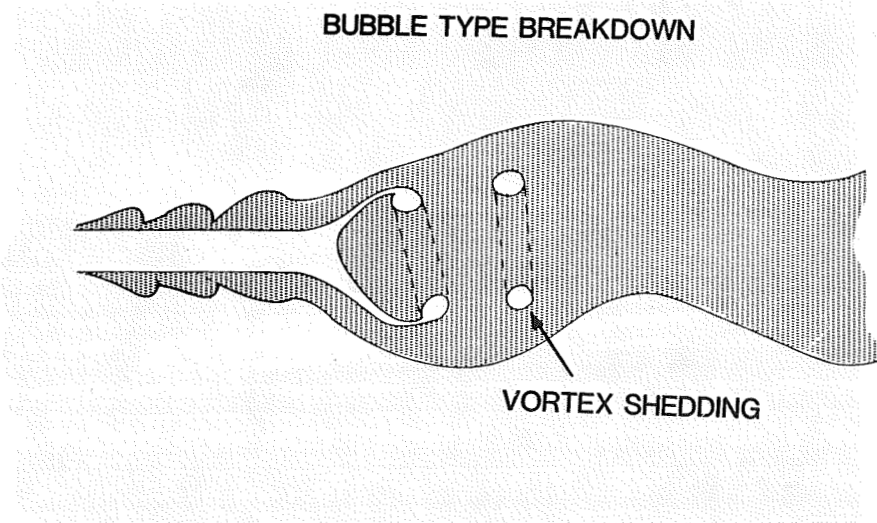


d. Longitudinal laser sheet cross section.
Sweep = 85 deg, Alpha = 40 deg, $V_{\infty} = 3$ m/s.

Figure 12. Concluded.



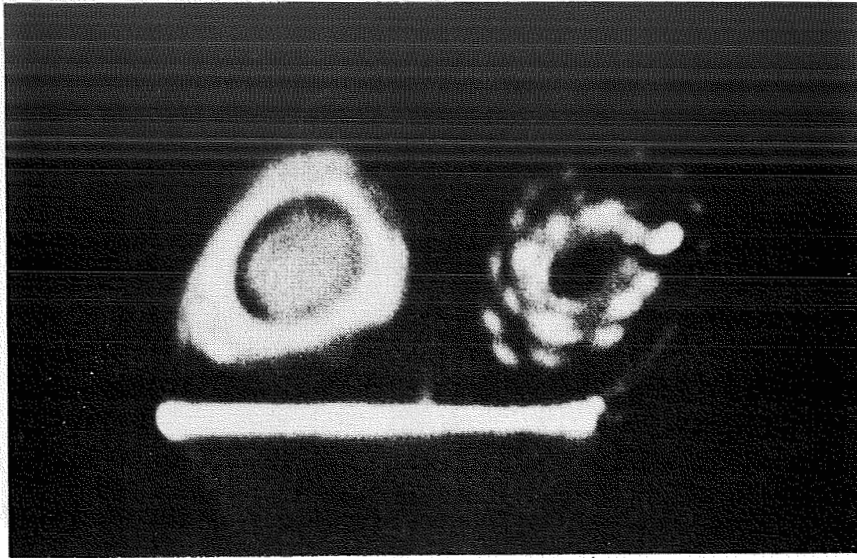
a. Enlargement from 16-mm movie frame. Bubble-type breakdown. Longitudinal cross section.



b. Schematic representation of bubble-type breakdown. Longitudinal cross section.

Figure 13. Longitudinal view of bubble-type breakdown.

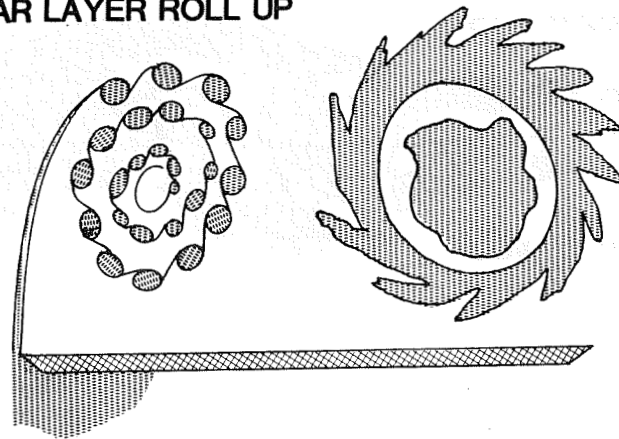
ORIGINAL PAGE IS
OF POOR QUALITY



- a. Enlargement from 16-mm movie frame. Bubble-type breakdown. Lateral cross section.

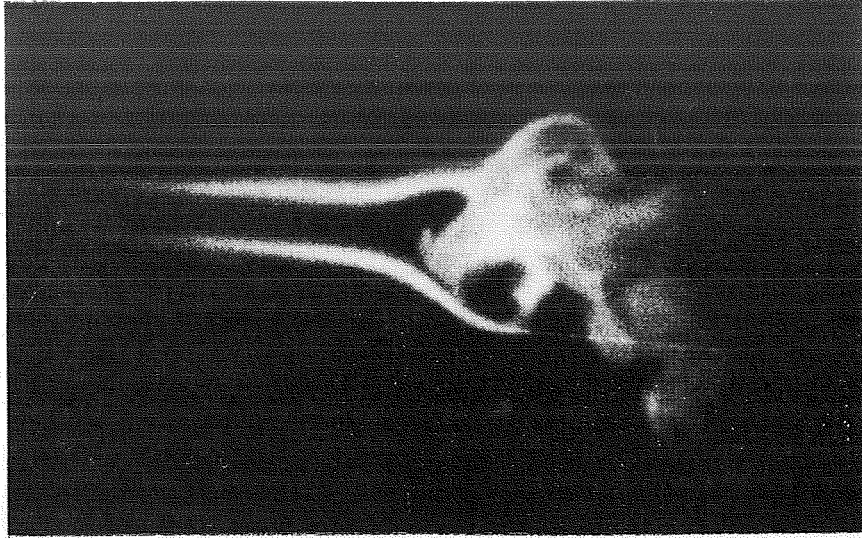
BUBBLE TYPE VORTEX BREAKDOWN

SHEAR LAYER ROLL UP



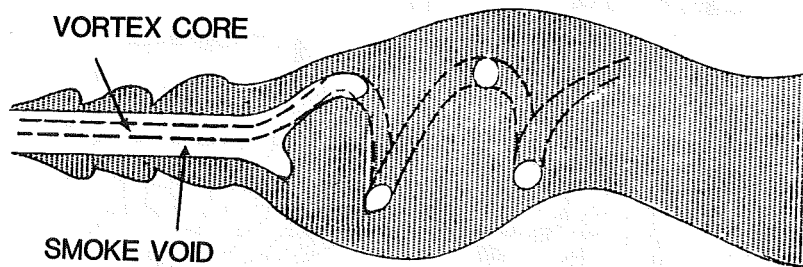
- b. Schematic representation of bubble-type breakdown. Lateral cross section.

Figure 14. Lateral view of bubble-type breakdown.



a. Enlargement from 16-mm movie frame. Spiral-type breakdown. Longitudinal cross section.

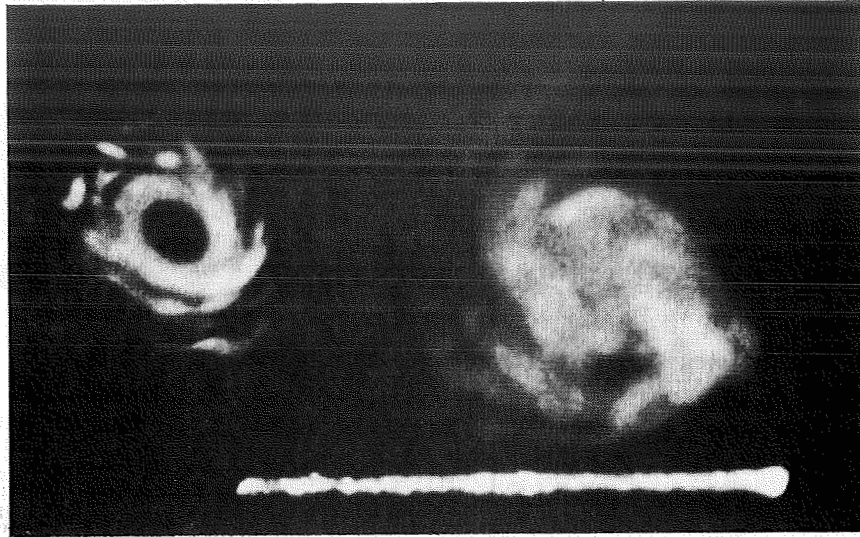
SPIRAL TYPE VORTEX BREAKDOWN



b. Schematic representation of spiral-type breakdown. Longitudinal cross section.

Figure 15. Longitudinal view of spiral-type breakdown.

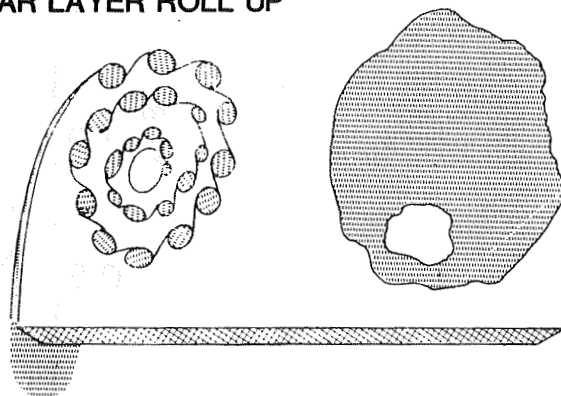
ORIGINAL PAGE IS
OF POOR QUALITY



- a. Enlargement from 16-mm movie frame.
Spiral-type breakdown. Lateral cross
section.

SHEAR LAYER ROLL UP

SPIRAL VORTEX BREAKDOWN



- b. Schematic representation of spiral-
type breakdown. Lateral cross section.

Figure 16. Lateral view of spiral-type breakdown.

DELTA WING L. E. VORTEX - AXIAL VELOCITY

Sweep Angle = 70 deg.
Angle of Attack = 30 deg.
U = Freestream Velocity = 9.1 m/sec.

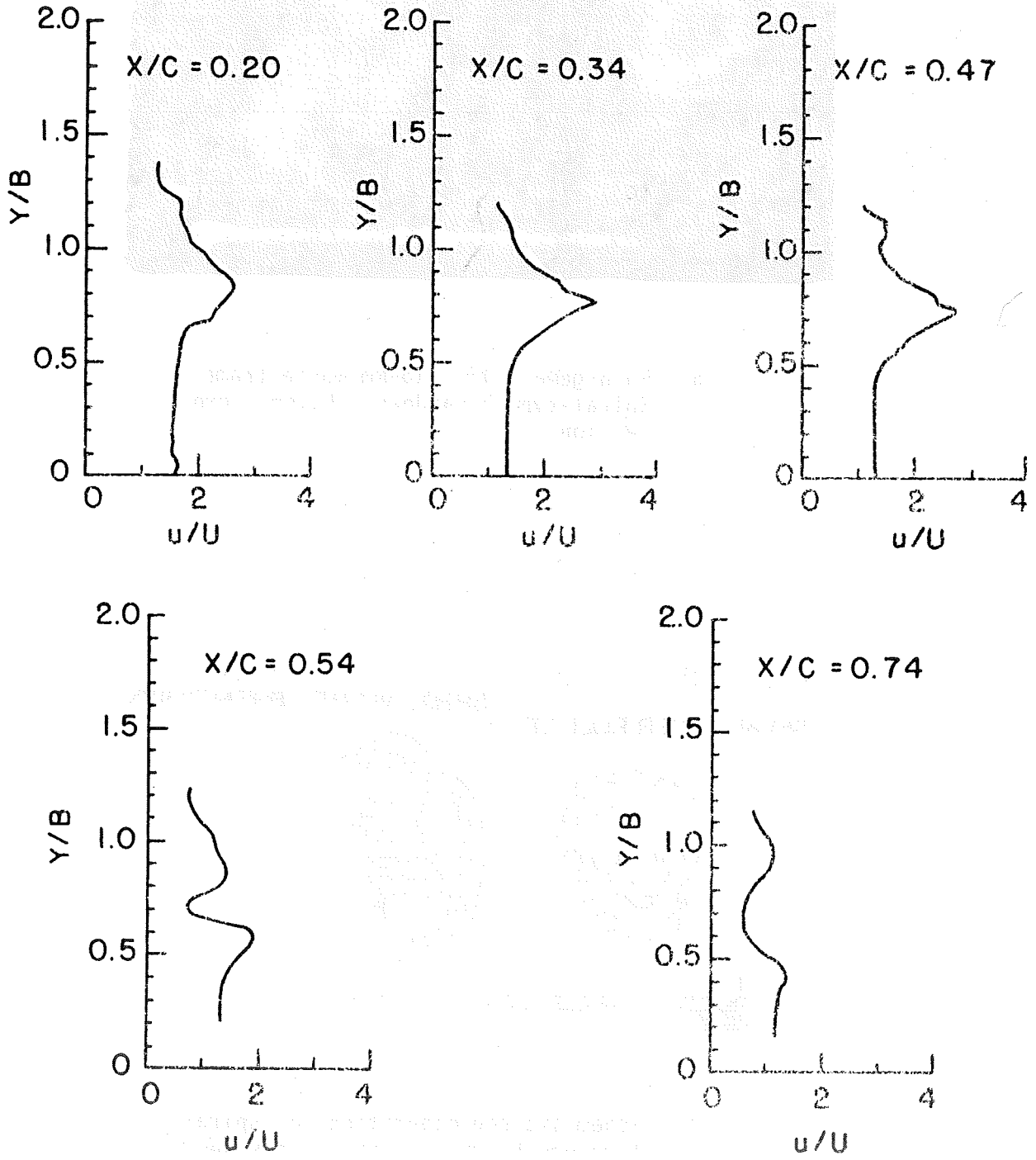


Figure 17. LDA measurements: axial velocity profiles.

DELTA WING L.E. VORTEX - SWIRL VELOCITY

Sweep Angle = 70 deg.

Angle of Attack = 30 deg.

U = Freestream Velocity = 9.1 m/sec.

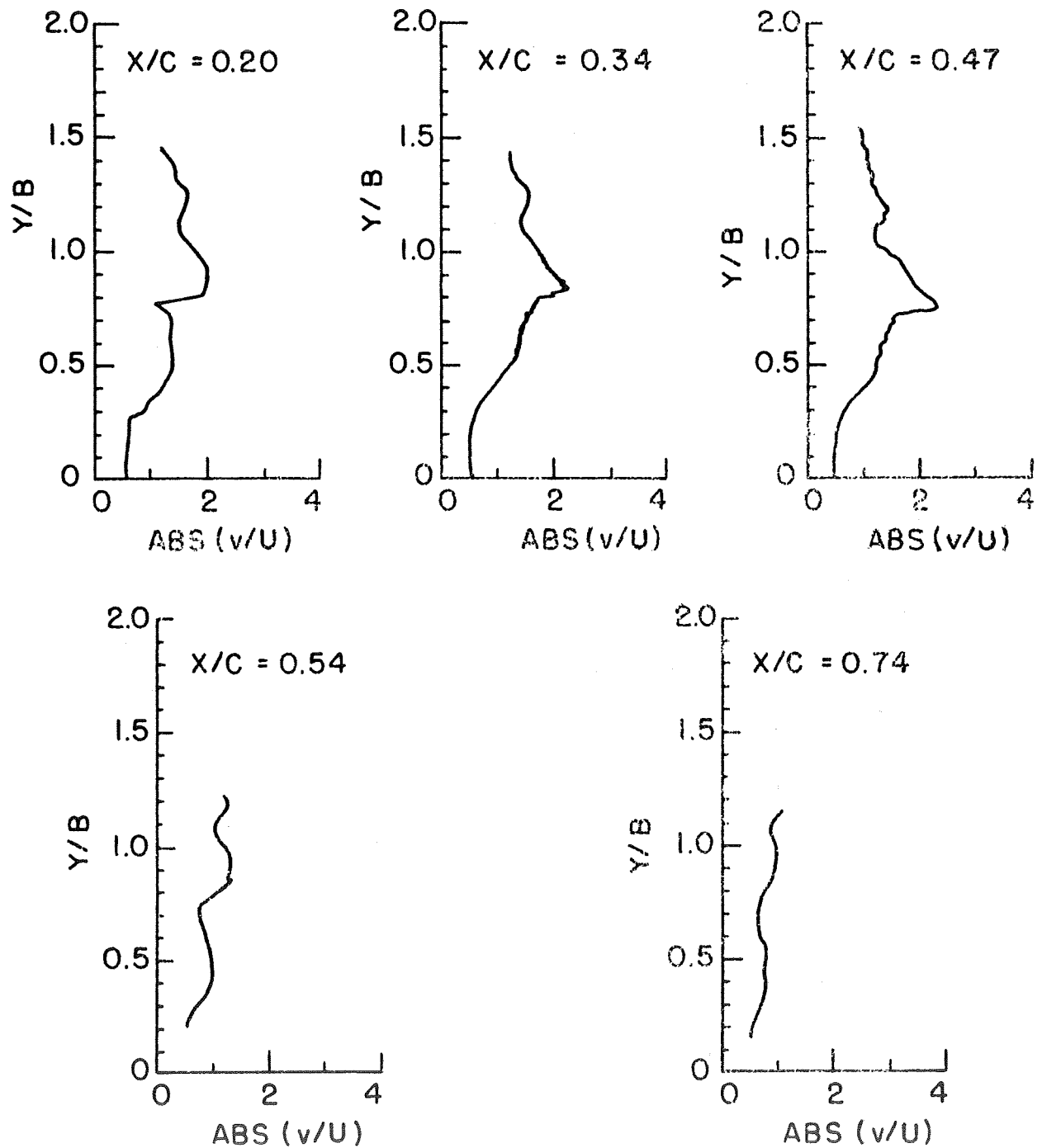


Figure 18. LDA measurements: swirl velocity profiles.